Catalysis Today 147S (2009) S41–S45

Contents lists available at ScienceDirect

Catalysis Today

journal homepage: www.elsevier.com/locate/cattod

Palladium supported on hierarchically macro–mesoporous titania for styrene hydrogenation

Tian-Ying Zeng, Zhi-Ming Zhou *, Jun Zhu, Zhen-Min Cheng, Pei-Qing Yuan, Wei-Kang Yuan

State Key Laboratory of Chemical Engineering, East China University of Science and Technology, Shanghai 200237, China

ARTICLE INFO

Article history:
Available online 3 August 2009

Keywords:
Titania
Hierarchical
Macroporous
Mesoporous
Catalyst
Hydrogenation

ABSTRACT

Hierarchically macro–mesoporous titania was synthesized by the simple dropwise addition of tetrabutyl titanate to an ammonia solution in the absence of surfactant molecules, and then calcined at different temperatures. The as-prepared titania was characterized by X-ray diffraction, N_2 adsorption–desorption analysis and scanning electron microscopy. The results showed that the hierarchically marcro–mesoporous structure of the titania was well preserved after calcination at 650 °C, indicating high thermal stability. The 500 °C calcined titania with the hierarchically bimodal pore network was impregnated with 0.5 wt.% of palladium and compared with 0.5 wt.% Pd/TiO_2 catalyst without such macrochannels. The novel macro–mesostructured Pd/TiO_2 catalyst exhibited higher catalytic activity for styrene hydrogenation due to the lower diffusion resistance of species inside the catalyst caused by the hierarchically macro–mesoporous bimodal structure.

1. Introduction

Pyrolysis gasoline (Pygas) is the byproduct of steam cracking of light naphatha in olefin plants. It contains a large quantity of aromatics such as benzene, toluene and xylene (BTX), and a small amount of unsaturated components such as olefins and dienes [1]. These unstable components prevent hydrodesulfurization of sulfur-containing compounds at high temperature. In order to recover BTX, the unsaturated components are converted by hydrogenation into saturated species before aromatics extraction [2–5]. Considering that the main component of such unsaturates is styrene, which is about 80–90 wt.% (mass percent) of the total amount of unsaturates, hydrogenation of styrene becomes an important reaction in Pygas post-treatment.

The pore-size distribution of the commercial catalysts for Pygas hydrogenation is normally between 4 and 20 nm [6]. This distribution is applicable in the short term, but in the long run, many mesopores in the catalyst will be blocked with gums formed by polymerization of styrene and dienes [7–9]. As a result, some active sites of the catalyst will be covered; meanwhile, diffusion resistance of species in these pores will increase dramatically. Both disadvantages will decrease the catalyst performance. However, if the residence time of reactants inside the catalyst can be shortened to some extent, the amount of gums formed will be reduced, and the catalyst performance will be kept for a longer time.

Hierarchically macro–mesoporous transition metal oxides such as TiO_2 and ZrO_2 have attracted considerable attention due to their potential technology applications [10–16]. The unique pore structure of such oxides, i.e., the monolithic macropores and the hierarchical structure, makes them high-potential supports and catalysts. Hierarchically macro–mesoporous TiO_2 has been found to be high efficient for photocatalytic oxidation decomposition of volatile organic compounds (VOCs) [17,18]. Hierarchically porous ZrO_2 has been used as catalyst support for VOCs catalytic oxidation [19,20]. However, to the best of our knowledge, this kind of metal oxides with the hierarchically macro–mesoporous structure has so far never been applied to other reaction types except for oxidation reactions. Here, we report that palladium supported on hierarchically macro–mesoporous TiO_2 can be used as an effective catalyst for styrene hydrogenation in Pygas post-treatment.

2. Experimental

2.1. Titania support preparation

The hierarchically ordered porous titania was prepared by a method very similar to that described by Collins et al. [21] except that no stirring was used in their work. In a typical synthesis, 3 mL of tetrabutyl titanate (TBOT) was added dropwise into 30 mL of an ammonia solution (pH 12) at room temperature with slow stirring (200 rpm) in the absence of surfactant molecules. After reaction for

* Corresponding author. Tel.: +86 21 6425 2230 fax: +86 21 6425 3528.
E-mail address: zmzhou@ecust.edu.cn (Z.-M. Zhou).

0920-5861/$ – see front matter © 2009 Elsevier B.V. All rights reserved.
doi:10.1016/j.cattod.2009.07.029

2 h, the precipitates formed were removed, rinsed with distilled water repeatedly, and then left to dry at room temperature for 24 h. The as-prepared samples were finally calcined in air at 350, 500, 650 and 800 °C for 5 h at a heating rate of 1 °C min^{-1}, individually.

2.2. Catalyst preparation

The palladium-supported catalyst with 0.5 wt.% metal loading was prepared by incipient-wetness impregnation of the aforementioned 500 °C calcined sample with palladium chlorite aqueous solution. The impregnated powders were then dried at 120 °C for 6 h, and finally calcined in air from room temperature to 500 °C (ramp of 1 °C min^{-1}) and kept at 500 °C for 5 h. The as-prepared catalyst was called Pd/TiO_2(macro–meso). Before the catalytic test, the catalyst was reduced in a flow of hydrogen at 200 °C for 2 h.

For comparison, palladium supported on a titania without such a macro–mesoporous structure, called Pd/TiO_2(ref), was also prepared by the same procedure as described above. The TiO_2(ref) support was synthesized by a method similar to that used for TiO_2(macro–meso) except that twice-distilled water (pH 7) replaced the ammonia solution. The as-prepared TiO_2(ref) was also calcined at 500 °C according to the above procedure before palladium impregnation.

2.3. Characterization

X-ray diffraction (XRD) patterns of the prepared samples were obtained on a Rigaku D/Max 2550 VB/PC diffractiometer with Cu Kα radiation scanning 2θ angles ranging from 10° and 80°. Nitrogen adsorption–desorption isotherms and the corresponding pore-size distributions were acquired at −196 °C on a Micromeritics ASAP 2020 M instrument. All the samples were degassed for 6 h at 190 °C and 1 mmHg prior to nitrogen adsorption measurements. The pore diameter and the pore-size distribution were determined by the DFT method for the sample without calcination and by the BJH method for other samples. According to the IUPAC classification [22], pores are divided into three types, i.e., macropores with a large diameter (>50 nm), mesopores with a middle diameter (2–50 nm) and micropores with a small diameter (<2 nm). The morphology and the macroporous array of the TiO_2 powders were examined with a JEOL JSM 6360 LV scanning electron microscope (SEM). Transmission electron microscope (TEM) samples were prepared by dispersing ground samples in ethanol with ultrasound and drying a drop on a carbon coated copper grid, and then observed on a JEOL JEM 2010 electron microscope with an accelerating voltage of 200 kV and a point resolution of 0.18 nm. Metal dispersions were measured by using CO pulse chemisorption on a Micromeritics AutoChem 2920 apparatus. The weighed catalysts were reduced in a mixture of 10% H_2/Ar (100 mL/min) at 200 °C for 2 h followed by a switch to helium (100 mL/min) for 20 min at 200 °C to remove adsorbed hydrogen. After the catalysts were cooled to 35 °C in a helium flow, carbon monoxide pulses were injected into the quartz reactor and the net volume of CO was monitored with a thermal conductivity detector (TCD). A chemisorption stoichiometry of one CO molecule per surface palladium atom was assumed.

Hydrogenation of styrene dissolved in the n-hexane solvent (styrene 8.5 wt.% and n-hexane 91.5 wt.%) was carried out in a stirred semi-batch reactor at total pressures of 2.0–4.0 MPa over a temperature range of 40–60 °C. Reaction products were analyzed by a gas chromatograph (HP 6890) equipped with a 30 m long capillary column (HP-5) and a flame ionization detector (FID). Ethylcyclohexane, the product of ethylbenzene hydrogenation, was not observed in this study. Detailed information on the experimental procedure was reported elsewhere [4].

3. Results and discussion

3.1. Physico-chemical characterization

Fig. 1 shows the SEM images of the TiO_2 powders without calcination. It is apparent that the macroporous channels are parallel to each other and perpendicular to the tangent of the outer surface. Similar structures have been observed by other groups [16–18,21]. By comparison of Fig. 1(a) with Fig. 1(b), one can see that smaller monolithic macrochannels were obtained with slow stirring (0.5–0.8 μm, Fig. 1(a)) than those without stirring (2–3 μm, Fig. 1(b)). In addition, the nitrogen adsorption–desorption measurements showed that the former sample had a larger specific surface area (305 m^2 g^{-1}) than the latter (267 m^2 g^{-1}). Therefore, from the viewpoint of catalyst preparation, the TiO_2 powder prepared under slow stirring is more suitable to be used as catalyst support.

As for the formation mechanism for the hierarchically macro–micro/mesoporous structure, several researchers [12,14,16,21] explored in this field. Among these studies, the mechanisms proposed by Deng et al. [12] and by Collins et al. [21] can explain the formation of the micro/mesopores and of the macropores, respectively. The formation of the smaller micro/mesopores is governed by the nanoparticle aggregation mechanism [12], while the spontaneous self-assembly mechanism [16,21] is responsible for the formation of the macropores. According to the model proposed by Collins et al. [21], when a TBOT droplet is introduced

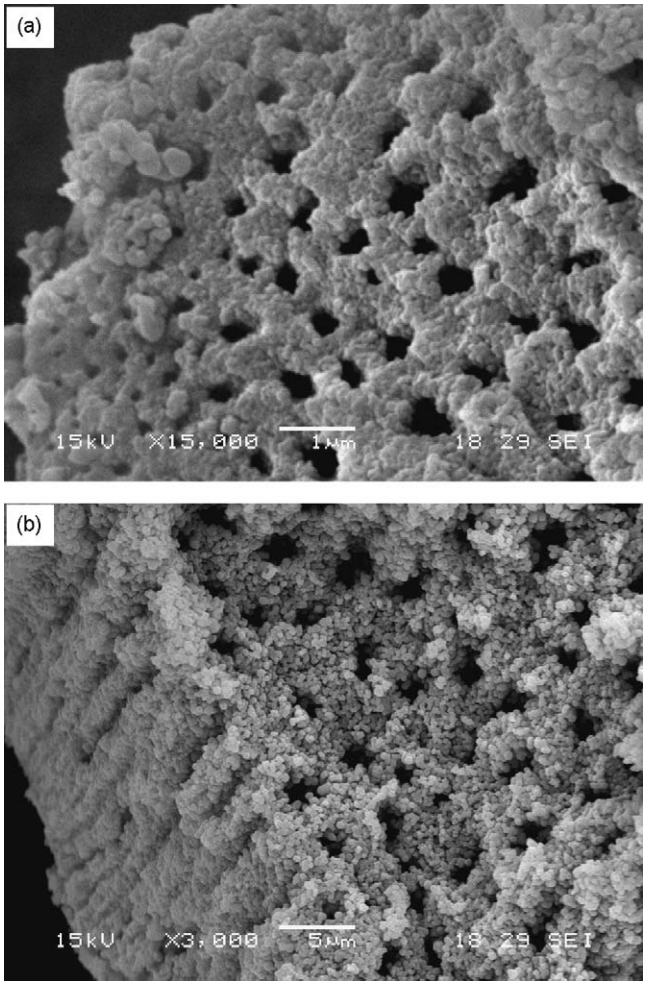

Fig. 1. SEM images of hierarchically macro–mesoporous TiO_2: (a) with slow stirring, scale bar = 1 μm; (b) without stirring, scale bar = 5 μm.

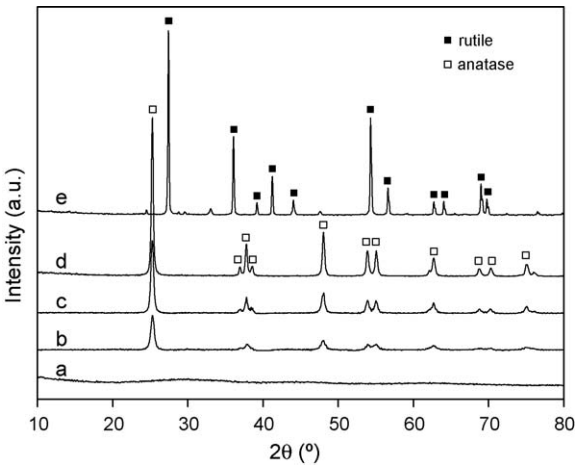

Fig. 2. XRD patterns of TiO_2 without calcination (a) and with calcination at (b) 350, (c) 500, (d) 650 and (e) 800 °C.

into the ammonia solution, a thin semipermeable titiania shell is simultaneouly formed at the outer surface of the droplet. The reaction front then proceeds inwardly, and the hydrolysis and condensation reactions occur in concert to produce the solid phase (TiO_2 nanoparticles) and the liquid phase (water and alcohol), which consequently results in the microphase-separated regions that generates the macroporous channels.

The XRD patterns of the TiO_2 samples with and without calcination are shown in Fig. 2. The as-prepared sample was in an amorphous phase (Fig. 2(a)). The samples after calcination at 350, 500 and 650 °C exhibited diffraction peaks assigned to the anatase phase (Fig. 2(b–d)), and these peaks became stronger and sharper with the increase in temperature. When the sample was further calcined up to 800 °C, the rutile phase was observed (Fig. 2(e)). Corresponding to 350, 500, 650 and 800 °C, the crystallite size of the calcined samples were 16.2, 19.5, 28.9 and 60.8 nm, respectively. The XRD results revealed that thermal treatment of the synthesized samples induced the growth of the crystallite size and subsequent phase transition.

The nitrogen adsorption–desorption isotherms of the TiO_2 samples and the corresponding pore-size distribution curves are presented in Fig. 3. For the as-prepared amorphous TiO_2 sample, the isotherm (Fig. 3(a)) exhibited high adsorption at low relative pressure, while the adsorption and desorption branches overlapped at high relative pressure. This indicated that the walls of the sample separating the macropores were in the framework of microporous structure, which was evidenced by its pore-size distribution shown in Fig. 3(b). Calcination treatment of the as-prepared sample at 350 °C resulted in the variation of the pore size from micropore to mesopore, and accompanying an increase in the calcination temperature, the pore size of the samples varied increasingly (Fig. 3(b)). As a result, the corresponding specific surface area together with the porosity gradually decreased, which can be directly seen from the decrease in volume adsorbed at high relative pressure (Fig. 3(a)). In contrast to the distinct variation of the mesopore size with the calcination temperature, the monolithic macroporous structure was well preserved and the diameters of such macropores were around 2–3 μm over a calcination temperature range of 350–650 °C (Fig. 4(b–d)).

The SEM images of the samples calcined at different temperatures (Fig. 4) as well as the XRD results (Fig. 2) indicate that the as-prepared hierarchically macro–mesoporous titania with the anatase phase possesses high thermal stability. This result is very exciting because high thermal stability is prerequisite to the catalyst support.

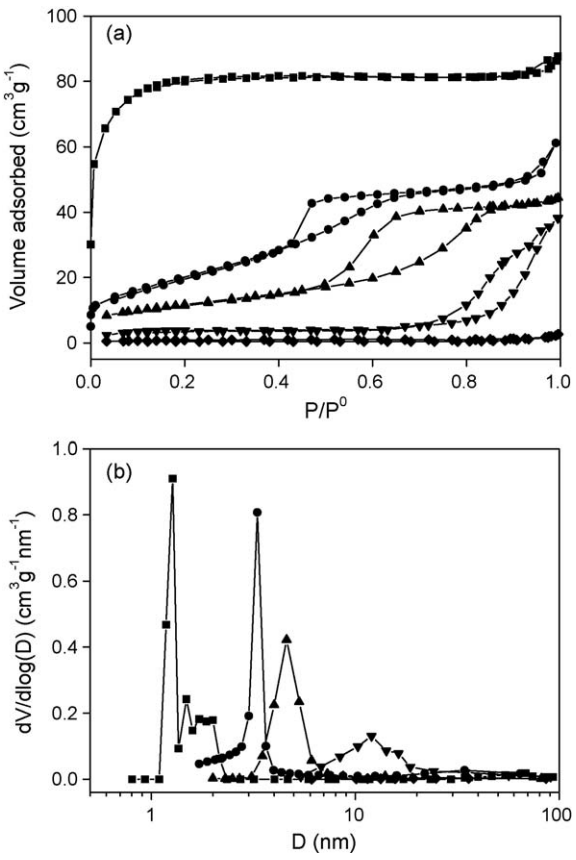

Fig. 3. N_2 adsorption–desorption isotherms (a) and corresponding pore-size distribution curves (b) of TiO_2 without calcination (■) and with calcination at 350 (●), 500 (▲), 650 (▼) and 800 °C (◆).

Fig. 5 shows the SEM micrographs of the TiO_2(ref) samples. It can be seen that there were no monolithic macrochannels in both the as-prepared (Fig. 5(a)) and the calcined TiO_2(ref) powders (Fig. 5(b)). This finding suggested that by using the above-mentioned synthesis method, the pH of the solution influenced the formation of the macrochannels. This result is in agreement with that obtained by Hakim and Shanks [16]. The average pore diameter of the calcined TiO_2(ref) was 4.8 nm, which approximated that of the 500 °C calcined TiO_2(macro–meso).

The palladium metallic particles for both Pd/TiO_2(ref) and Pd/TiO_2(macro–meso) were well dispersed by TEM measurement (TEM images are not shown here), and the average palladium size for both catalysts was almost the same (*ca.* 3 nm). Values of palladium dispersion obtained from CO chemisorption were 17.3% and 15.1% for Pd/TiO_2(macro–meso) and Pd/TiO_2(ref), respectively.

3.2. Catalytic activity

Catalytic activity data of the two catalysts for styrene hydrogenation are compared in Fig. 6. Apparently, the Pd/TiO_2(macro–meso) catalyst exhibited the higher catalytic activity. Taking the reaction occurring at 40 °C and 2.0 MPa as an example (see Fig. 6(a)), the initial reaction rates for the Pd/TiO_2(ref) and Pd/TiO_2(macro–meso) catalysts were equal to 0.037 and 0.061 mol g^{-1} h^{-1}, respectively.

This catalytic behavior can be attributed to the much lower internal diffusion limitation of species in Pd/TiO_2(macro–meso) than that in Pd/TiO_2(ref). Firstly, the parallel-arranged macroporous channels can greatly reduce diffusion resistance of species from the outer surface to the inner surface of the Pd/TiO_2(macro–meso) catalyst [23,24]. Secondly, the narrow width of the

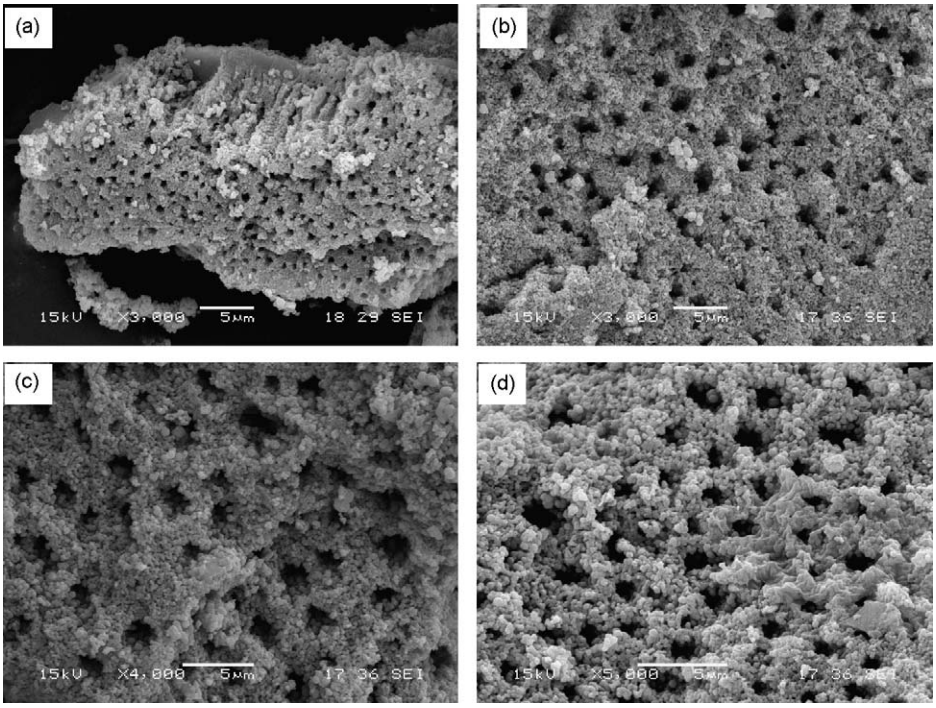

Fig. 4. SEM images of TiO_2 without calcination (a) and with calcination at (b) 350, (c) 500 and (d) 650 °C. (Scale bar: 5 μm.)

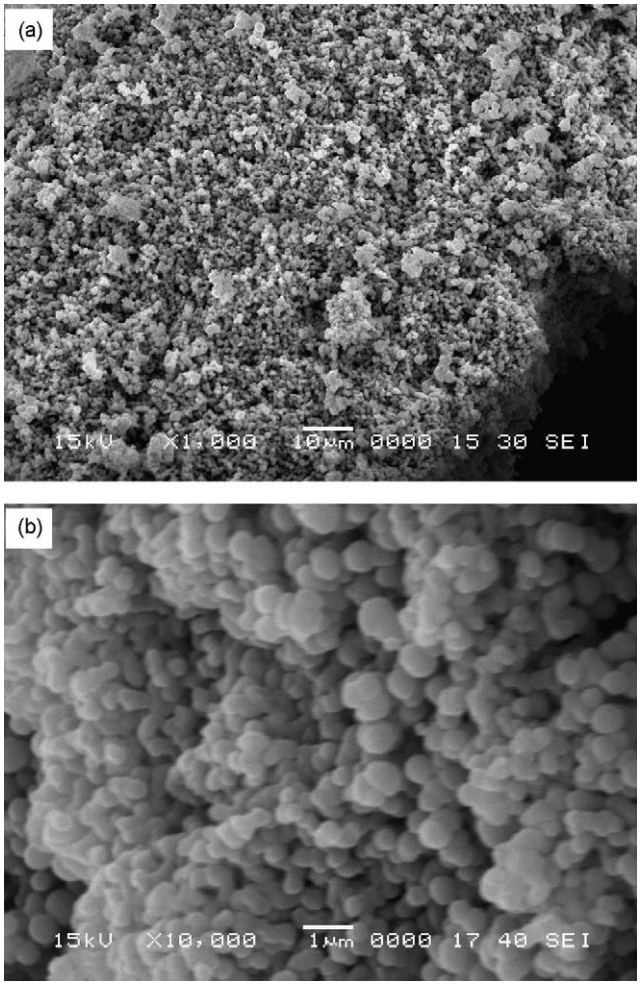

Fig. 5. SEM images of TiO_2(ref): (a) without calcination (scale bar = 10 μm); (b) with calcination at 500 °C (scale bar = 1 μm).

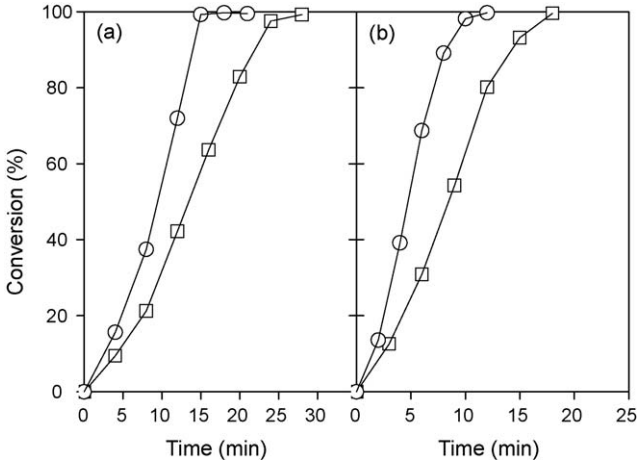

Fig. 6. Styrene conversion versus time for different catalysts: (○) Pd/TiO_2(macro–meso); (□) Pd/TiO_2(ref); (a) T = 40 °C, P = 2.0 MPa; (b) T = 50 °C, P = 3.0 MPa.

mesostructured porous walls (2–3 μm) can shorten the diffusion distance of reactants to the active sites and consequently decrease the concentration gradient of species, which in turn increases the reaction rate. Moreover, both the macroporous channels and the narrow walls are beneficial for reducing the residence time of styrene within the catalyst, resulting in few gums formed and a long catalyst life.

4. Conclusions

A novel palladium catalyst supported on hierarchically macro–mesoporous titania has been successfully prepared and applied to styrene hydrogenation. The hierarchically macro–mesoporous structure plays an important role in reducing the diffusion resistance of species inside the catalyst, which directly results in the higher catalytic activity of the novel catalyst in styrene hydrogenation in comparison with the palladium supported on the mesoporous titania without the monolithic macrochannels. It may

be expected that this novel catalyst will be an ideal catalyst for hydrogenation of pyrolysis gasoline in olefin plants.

Acknowledgements

Financial supports from the Natural Science Foundation of China (No. 20706018), the National High Technology Research and Development Program of China (No. 2008AA05Z405) and Program for Changjiang Scholars and Innovative Research Team in University (No. IRT0721) are gratefully acknowledged.

References

[1] Z.M. Zhou, Z.M. Cheng, D. Yang, X. Zhou, W.K. Yuan, J. Chem. Eng. Data 51 (2006) 972.
[2] Y.M. Cheng, J.R. Chang, J.C. Wu, Appl. Catal. 24 (1986) 273.
[3] N. Mostoufi, R. Sotudeh-Gharebagh, M. Ahmadpour, J. Eyvani, Chem. Eng. Technol. 28 (2005) 174.
[4] Z.M. Zhou, Z.M. Cheng, Y.N. Cao, J.C. Zhang, D. Yang, W.K. Yuan, Chem. Eng. Technol. 30 (2007) 105.
[5] A.B. Gaspar, G.R. Santos, R.S. Costa, M.A.P. Silva, Catal. Today 133–135 (2008) 400.
[6] S.Q. Li, X.T. Men, G.S. Liu, S.Q. Liang, X.G. Zhang, US Patent 6,576,586 (2003).
[7] T.A. Nijhuis, F.M. Dautzenberg, J.A. Moulijn, Chem. Eng. Sci. 58 (2003) 1113.
[8] M.P. Kaminsky, US Patent, 6,949,686 (2005).
[9] D.I. Enache, P. Landon, C.M. Lok, S.D. Pollington, E.H. Stitt, Ind. Eng. Chem. Res. 44 (2005) 9431.
[10] J.L. Blin, A. Léonard, Z.Y. Yuan, L. Gigot, A. Vantomme, A.K. Cheetham, B.L. Su, Angew. Chem. Int. Ed. 42 (2003) 2872.
[11] B.L. Su, A. Léonard, Z.Y. Yuan, C. R. Chimie 8 (2005) 713.
[12] W.H. Deng, B.H. Shanks, Chem. Mater. 17 (2005) 3092.
[13] A. Léonard, A. Vantomme, C. Bouvy, N. Moniotte, P. Mariaulle, B.L. Su, Nanopages 1 (2006) 1.
[14] A. Vantomme, A. Léonard, Z.Y. Yuan, B.L. Su, Colloids Surf. A: Physicochem. Eng. Aspects 300 (2007) 70.
[15] A. Léonard, A. Vantomme, B.L. Su, in: G.Z. Cao, C.J. Brinker (Eds.), Annual Review of Nano Research, vol. 2, World Scientific Publishing Co. Pte. Ltd., Singapore, 2008 p. 393 (Chapter 9).
[16] S.H. Hakim, B.H. Shanks, Chem. Mater. 21 (2009) 2027.
[17] X.C. Wang, J.C. Yu, C.M. Ho, Y.D. Hou, X.Z. Fu, Langmuir 21 (2005) 2552.
[18] J.G. Yu, Y.R. Su, B. Cheng, Adv. Funct. Mater. 17 (2007) 1984.
[19] H.L. Tidahy, S. Siffert, J.F. Lamonier, E.A. Zhilinskaya, A. Aboukaïs, Z.Y. Yuan, A. Vantomme, B.L. Su, X. Canet, G.D. Weireld, M. Frère, T.B. N'Guyen, J.M. Giraudon, G. Leclercq, Appl. Catal. A: Gen. 310 (2006) 61.
[20] H.L. Tidahy, M. Hosseni, S. Siffert, R. Cousin, J.F. Lamonier, A. Aboukaïs, B.L. Su, J.M. Giraudon, G. Leclercq, Catal. Today 137 (2008) 335.
[21] A. Collins, D. Carriazo, S.A. Davis, S. Mann, Chem. Commun. (2004) 568.
[22] K.S.W. Sing, D.H. Everett, R.A.W. Haul, L. Moscou, R.A. Pierotti, J. Rouquérol, T. Siemieniewska, Pure Appl. Chem. 57 (1985) 603.
[23] T. Doğu, Ind. Eng. Chem. Res. 37 (1998) 2158.
[24] J.A. Delgado, A.E. Rodrigues, Ind. Eng. Chem. Res. 40 (2001) 2289.